JOURNAL OF GEOPHYSICAL RESEARCH, VOL. 100, NO. C7, PAGES 13,441–13,453, JULY 15, 1995

Antarctic Intermediate Water circulation in the tropical and subtropical South Atlantic

Toshio Suga[1] and Lynne D. Talley

Scripps Institution of Oceanography, University of California, San Diego, La Jolla

Abstract. Recent hydrographic data from the South Atlantic Ventilation Experiment cruises and others are combined with historical data and used to map the isopycnal properties corresponding to the Antarctic Intermediate Water (AAIW) in the Atlantic Ocean. The low salinity of the AAIW extends eastward across the South Atlantic just south of the equator (3–4°S). Evidence of a weak eastward flow just north of the equator (1–2°N) is also shown. Lateral and vertical homogenization of properties in the AAIW is found at the equator between 2°S and 2°N; there is no clear zonal gradient in salinity just along the equator. These observations suggest enhanced mixing within the equatorial baroclinic deformation radius. The South Atlantic tropical gyre is shown to consist of the following three cells: one cyclonic cell centered at about 7°S, another centered at about 19°S in the west and 23°S in the east, and one anticyclonic cell centered at about 13°S. These cells are associated with a westward extension at 10°S of high salinity and low oxygen which originates in the eastern tropical South Atlantic and a front in these properties at about 15°S in the west and about 20°S in the east.

1. Introduction

Antarctic Intermediate Water (AAIW) spreads from the subantarctic region to the northern hemisphere in all three oceans: the Atlantic [*Wüst*, 1935; *Tsuchiya*, 1989], the Indian [*Taft*, 1963], and the Pacific [*Reid*, 1965; *Tsuchiya*, 1991]. AAIW has been considered traditionally to be formed by mixing across the Antarctic Polar Front [e.g., *Wüst*, 1935; *Molinelli*, 1981; *Piola and Georgi*, 1982], while *McCartney* [1977, 1982] proposed that the coldest Subantarctic Mode Water formed by convective overturning in the southeastern Pacific is the major source of AAIW. Several authors have discussed its circulation in each ocean since *Wüst* [1935] showed its northward spreading in the Atlantic Ocean by tracing the intermediate salinity minimum which characterizes AAIW in the southern hemisphere oceans. Recently, much attention has been drawn to interocean exchange of AAIW, which is part of the global meridional circulation cell associated with the formation of North Atlantic Deep Water (NADW) [e.g., *Rintoul*, 1991; *Gordon et al.*, 1992; *Fine*, 1993]. *Rintoul* [1991] used an inverse calculation to conclude that a surplus of AAIW is carried into the South Atlantic through Drake Passage and is compensated by a surplus of deep and bottom water leaving the basin south of Africa; the Atlantic as a whole converts intermediate water into deep and bottom water.

The circulation of AAIW in the Atlantic Ocean is particularly interesting in the context of the global cell because AAIW spreading into the North Atlantic can be a major warm source of NADW as mentioned above [*Broecker and Takahashi*, 1981; *Gordon and Piola*, 1983; *Rintoul*, 1991; *Gordon et al.*, 1992]. Owing to this overturning cell, the meridional heat transport in the midlatitude South Atlantic is equatorward rather than poleward. *Rintoul* [1991] showed an overturning cell of 17 Sv at 32°S which carries an equatorward heat flux of 0.25 PW. Relevant to its northward spreading in the South Atlantic, *Wüst* [1935] proposed continuous northward flow along the western boundary from the Falkland Current to the equator. Other studies [e.g., *Taft*, 1963; *Buscaglia*, 1971; *Piola and Georgi*, 1982; *Warner and Weiss*, 1992] suggested that AAIW flows northward along the western boundary up to 40°S, flows eastward, northward, and westward around the anticyclonic subtropical gyre, and then reenters the western boundary region flowing northward. *Rintoul*'s [1991] inverse calculation, however, suggested that northward flow of AAIW as part of the Brazil Current recirculation is also important along with the path around the subtropical gyre. Examining a series of recent sections across the western boundary between 38°S and 27°S, *Zemba* [1991] concluded that most of the AAIW flows around the subtropical gyre, while a relatively small part flows continuously northward along the western boundary as an intermediate boundary current under the southward flowing Brazil Current, and another small part flows northward in the return flow of the Brazil Current. *Wüst* [1935] inferred that part of the AAIW reaching the equator enters the North Atlantic in the western boundary current and part turns eastward just south of the equator. *Reid* [1994] indicated that AAIW crosses the equator along the western boundary based on adjusted steric height and isopycnal maps. *Richardson and Schmitz* [1993] showed mean northward velocity at 800 m along the western boundary from the equator to 11°N using SOFAR floats. AAIW in the North Atlantic can be traced as far north as 60°N following the path of the Gulf Stream–North Atlantic Current as a silica maximum [*Tsuchiya*, 1989], even though its low-salinity signature becomes obscure north of about 20°N.

The circulation of AAIW in the tropical South Atlantic has

[1]Permanently at Department of Geophysics, Graduate School of Science, Tohoku University, Sendai, Japan.

Paper number 95JC00858.
0148-0227/95/95JC-00858$05.00

not been described as thoroughly as elsewhere in the Atlantic. However, the tropical South Atlantic is important in modifying the properties of AAIW entering the North Atlantic because substantial alteration of properties in the water column, including AAIW, occurs in the cyclonic subequatorial gyre [*Reid*, 1989; *Gordon and Bosley*, 1991; *Tsuchiya et al.*, 1994]. In the eastern part of this gyre, off Africa, AAIW oxygen is greatly decreased and nitrate and phosphate are increased due to local consumption of oxygen [*Reid*, 1989]. *Tsuchiya et al.* [1994] suggested a complicated pattern of eastward and westward flows of AAIW near the equator based on the property distributions in the section along 25°W. These zonal flows probably facilitate alteration of AAIW in the tropical South Atlantic, which then crosses the equator into the North Atlantic.

Concerning the influence of the Indian Ocean on AAIW in the Atlantic, *Gordon et al.* [1992] suggested that considerable exchange of water occurs between the South Atlantic and Indian Ocean. They estimated that AAIW in the northwestward flowing Benguela Current along the northeastern rim of the subtropical gyre is a 50/50 mix of South Atlantic AAIW with Indian Ocean AAIW.

Recently, extensive modern hydrographic data, including those from the South Atlantic Ventilation Experiment (SAVE) and a section along 25°W, have been accumulated in the South Atlantic. These new data enable us to investigate in more detail the circulation path of AAIW in the tropical and subtropical South Atlantic, with reexamination of the features of its circulation discussed in the previous studies; this will give an essential background for quantitative estimation of AAIW transport and conversion in the context of the global cell. In section 2 the circulation pattern of AAIW in the South Atlantic is discussed based on the isopycnal maps, and its detailed features in the subequatorial and equatorial South Atlantic are presented in section 3.

2. Isopycnal Maps

All of the SAVE and 25°W data [*Scripps Institution of Oceanography*, 1992a, b, c] and other new data were combined with the historical data used by *Reid* [1989]. For mapping purposes, bottle data were used. Horizontal and vertical resolution along the modern sections apparent in the isopycnal maps has been excellent, with close station spacing in the boundary current regions sufficient for resolving narrow boundary currents and with vertical resolution which specifically samples the AAIW layer.

Along 25°W, *Tsuchiya et al.* [1994] showed that the AAIW salinity minimum is centered at about $27.15\sigma_\theta$ south of about 40°S and becomes denser equatorward, centered at about $27.2\sigma_\theta$ between 40°S and 20°S and at about $27.3\sigma_\theta$ north of 20°S. The isopycnal surface of $27.3\sigma_\theta$ was chosen for the present study, which coincides with the intermediate salinity minimum in most of the subtropical, subequatorial, and equatorial South Atlantic. This isopycnal corresponds to $31.938\ \sigma_1$ chosen by *Reid* [1989, 1994] for his isopycnal maps to represent the AAIW in the South Atlantic. The isopycnal almost outcrops near 60°S (Figure 1). It is deepest, below 1000 m, in the subtropical gyre near 30–40°S and becomes shallower to the north. North of about 20°S, it is slightly shallower than 800 m and rather flat.

Maps of salinity and oxygen at $27.3\sigma_\theta$ (Figures 2 and 3) suggest that there are three western boundary current regimes in the South Atlantic. The southernmost, from the subantarctic region to 20–25°S, has a very narrow western boundary current stretching northward with low salinity and high oxygen; offshore, lies the more saline, lower-oxygen Brazil Current, and farther offshore, the interior gyre values are similar to those of the narrow western boundary current. The middle regime, between 20°S and 10°S, has a broad western region of low salinity, which has probably entered from the east after being carried around the anticyclonic subtropical gyre; this is considered by most authors to be the major source of AAIW flowing northward along the western boundary in this region and, ultimately, the source of AAIW crossing the equator. The northernmost region, north of 10°S, has a narrow western boundary current similar to that of the southern region. Acceleration potential at $27.3\sigma_\theta$ relative to 3000 dbar (Figure 4) somewhat contradicts this isopycnal property view; a northward western boundary current is apparent in Figure 4 only in the middle regime. However, Figure 4 shows that the zonal flow east of the northern and southern regimes is eastward and the dominant western boundary current southward, whereas in the middle regime the interior flow is westward and the western boundary flow northward. The narrow AAIW tongues in the southern and northern regimes are inshore of the dominant western boundary currents. They are absent in the acceleration potential relative to 3000 dbar because the bottom depth under the narrow currents is shallower than 3000 dbar.

Thus the property maps and acceleration potential support the view that a portion of the AAIW is advected northward along the western boundary [*Wüst*, 1935; *Zemba*, 1991] but that most of the AAIW which enters the tropics comes from the flow around the subtropical gyre [*Zemba*, 1991]. The northward recirculation of the Brazil Current apparent in Figure 4 has a local effect on AAIW properties, as discussed by *Zemba* [1991], but is difficult to show in the isopycnal properties in Figures 2 and 3.

Isopycnic potential vorticity ($(f/\rho)(\partial\rho/\partial z)$) is expected to be homogenized within gyres if the isopycnal does not outcrop. *Keffer*'s [1985] potential vorticity for the layer $27.0\sigma_\theta$ to $27.3\sigma_\theta$ shows low potential vorticity on the south side of the subtropical gyre and high potential vorticity on the north side. North of 20°S, in the tropics, it has a zonal pattern dominated by the variation in Coriolis parameter (the beta effect). Potential vorticity for $27.3\sigma_\theta$ (Figure 5) is calculated using a much smaller density interval of $0.05\sigma_\theta$ in order to map it more locally in the vertical. As in the work by Keffer, in the tropics it is dominated by the beta effect. In the subtropical gyre we find that it appears more completely homogenized than Keffer did, although there are patches of high potential vorticity on the north side of the subtropical gyre, which appear to originate from the high potential vorticity in the Agulhas retroflection region. The somewhat higher potential vorticity on the north side of the subtropical gyre suggests that AAIW in the South Atlantic can be affected by water from the Indian Ocean, which is consistent with the hypothesis of input of AAIW from the Indian Ocean [*Gordon et al.*, 1992]. *Reid* [1989] also indicates that high silica, indicating Indian Ocean origin, extends from the south of Africa to the northwest. On the other hand, *Rintoul* [1991] found no net transfer of AAIW from the Indian Ocean to the Atlantic Ocean, suggesting that even though Indian Ocean AAIW enters the Atlantic from the Agulhas, the same

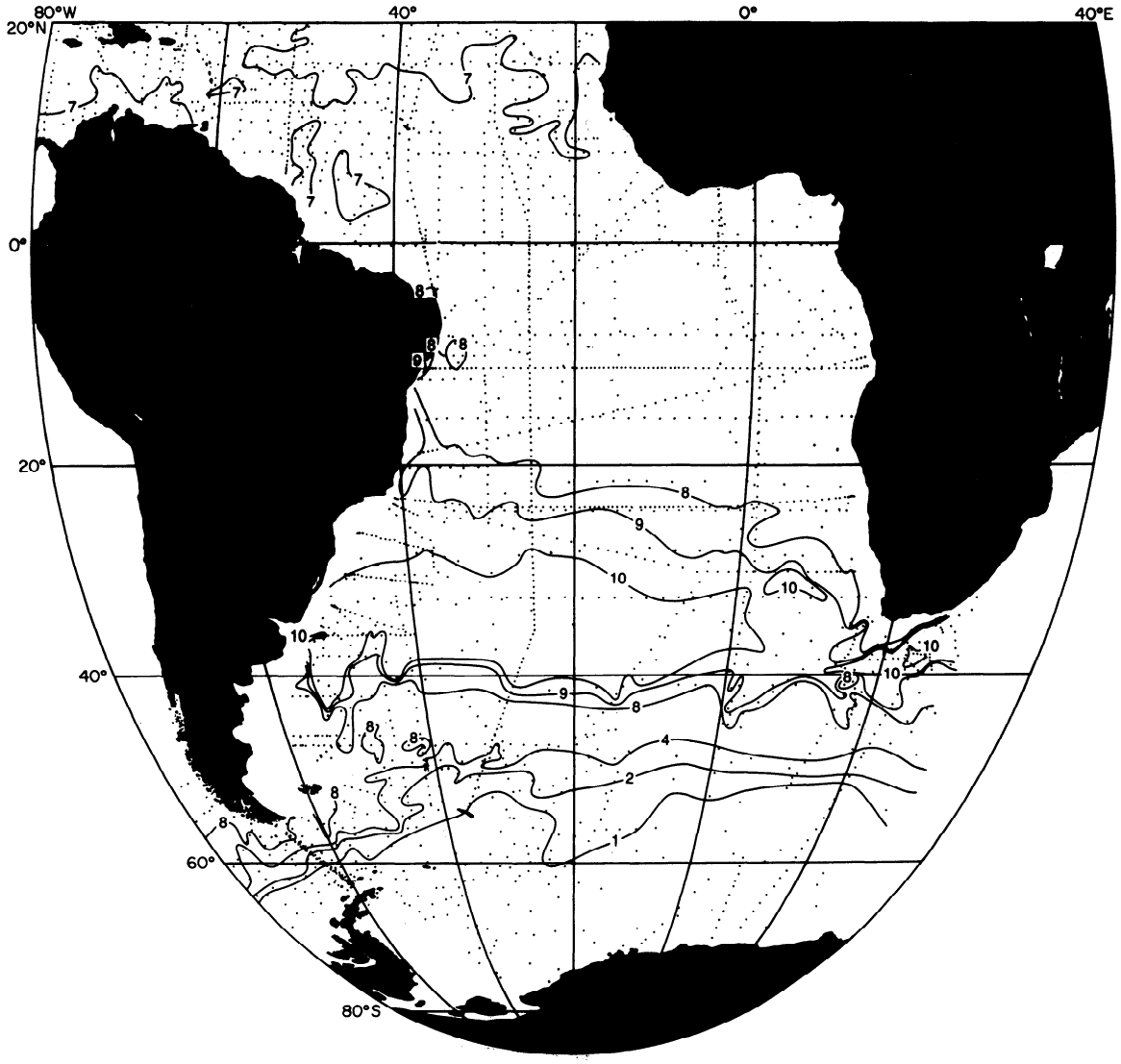

Figure 1. Depth (10^2 m) of the $27.3\sigma_\theta$ isopycnal.

amount flows in the other direction, probably in the Antarctic Circumpolar Current [*Gordon et al.*, 1992].

In the tropics a low-salinity and high-oxygen tongue extends eastward from the western boundary at 3–4°S and almost reaches to the eastern boundary (Figures 2 and 3). This pattern reflects eastward flow of AAIW south of the equator [*Wüst*, 1935] and *Reid*'s [1989] adjusted steric height at 800 dbar, in which broad eastward flow is shown schematically. A similar low-salinity tongue also appears on the $27.2\sigma_\theta$ surface based on the same data set as used here [*Tsuchiya et al.*, 1994]. Another much weaker low-salinity tongue extends eastward from the western boundary at 1–2°N, and a slight meridional minimum of salinity can be seen as far east as about 25°W, suggesting eastward flow of AAIW just north of the equator. The eastward flow at the middepth north of the equator was also indicated by *Reid*'s [1978] dynamic topography map at 1000 dbar relative to 2000 dbar. The tracer fields near the equator will be discussed in detail in the section 3.

Low oxygen (Figure 3) and high nitrate (not shown) are centered at 10°S near the eastern boundary. These lateral extrema have been explained as a result of fallout and regeneration of materials from the euphotic layer in the subequatorial gyre which has cyclonic flow and upwelling [*Reid*, 1989]. There is also an area of high salinity roughly coinciding with the region of low oxygen and high nitrate (Figure 2). A similar pattern was shown at $27.2\sigma_\theta$ by *Tsuchiya et al.* [1994]. As *Gordon and Bosley* [1991] and *Tsuchiya et al.* [1994] suggested, this high salinity indicates vertical mixing in this region along with the consumption of oxygen. The low oxygen, high nitrate, and high salinity then extend westward almost across the basin, suggesting westward flow centered at about 10°S. These westward tongues are more obvious in the present maps but are also evident in previous maps [*Wüst*, 1935; *Reid*, 1989].

A front in salinity and oxygen is found tilted from about 25°S in the west to 30°S in the east. This is the boundary between the subtropical and the subequatorial gyres according to, for example, the map of adjusted steric height at 800 dbar by *Reid* [1989, Figure 17] and extends vertically down through the Circumpolar and North Atlantic Deep Water [*Tsuchiya et al.*, 1994]. Another front appears at about 15°S

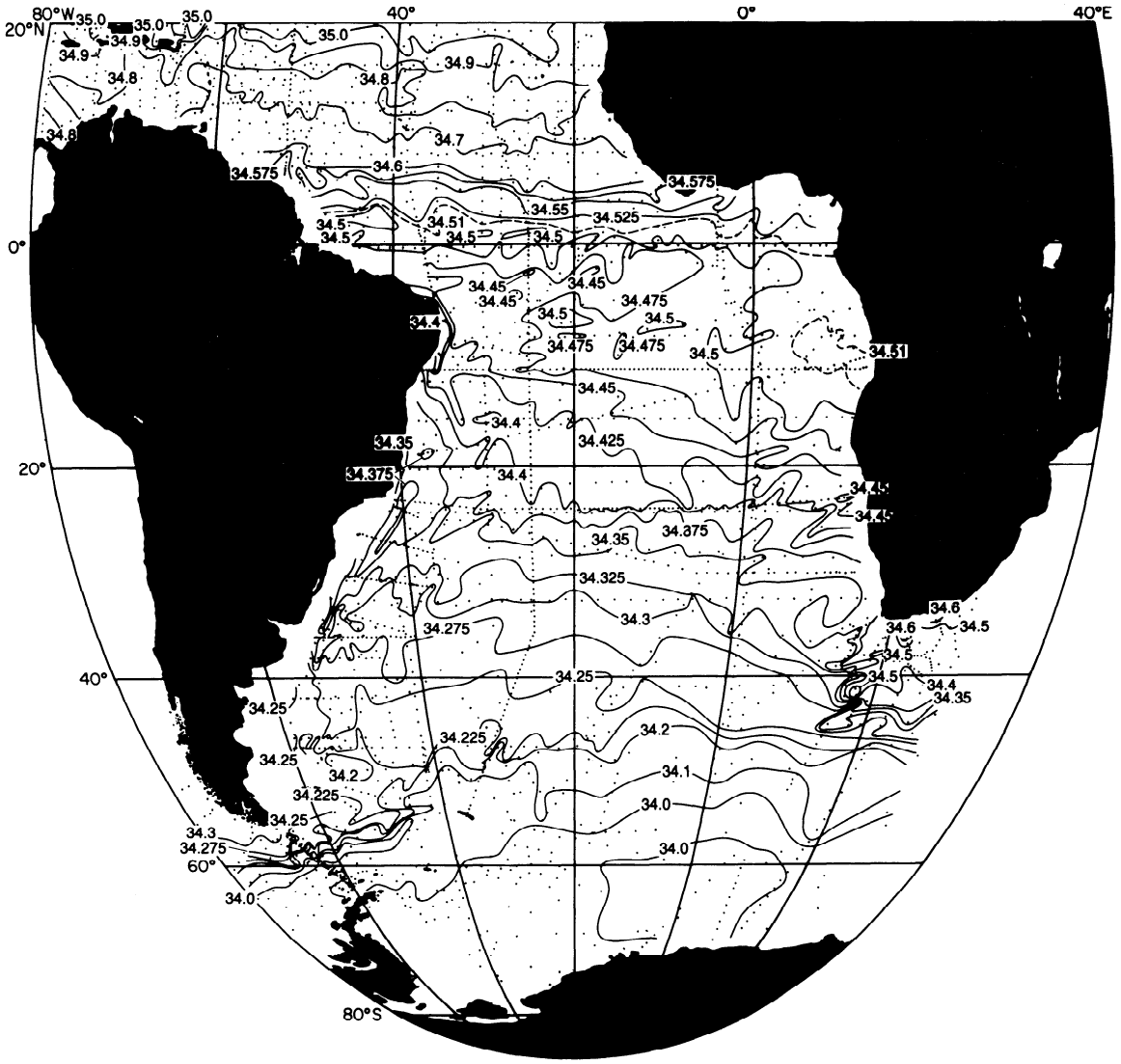

Figure 2. Salinity (practical salinity units) on the $27.3\sigma_\theta$ isopycnal.

in the west and 20°S in the east, running northwest to southeast, in the subequatorial gyre.

Acceleration potential at $27.3\sigma_\theta$ is calculated with respect to 3000 dbar (Figure 4). Since the flow at 3000 dbar by *Reid* [1989] north of 20°S is not very strong and would not eliminate major features in the present map completely it appears safe to choose the 3000-dbar surface as a zero reference level for at least the subequatorial gyre. The consistency of the features in the acceleration potential with the tracer fields in the subequatorial gyre also supports this use. The flow pattern in the anticyclonic subtropical gyre centered at 35°S is much the same as in the previous maps [e.g., *Reid*, 1989]. The pattern in the subequatorial gyre, however, is considerably different from the previous ones. A ridge in acceleration potential ($>1.8 \times 10$ m^2 s^{-2}) extends from the eastern boundary westward to 30°W between 10°S and 15°S, splitting the cyclonic subequatorial gyre into two parts. Consequently, the subequatorial gyre consists of the following three cells: one cyclonic cell centered at about 7°S, another centered at about 19°S in the west and 23°S in the east, and one anticyclonic cell centered at about 13°S. The westward flow on the northern side of the anticyclonic cell possibly accounts for the low-oxygen, high-salinity, and high-nitrate tongue extending westward from the eastern boundary, filling the cell with water influenced by the consumption of oxygen and vertical mixing off Africa. The eastward flow at the southern side of the cell corresponds well with the front in salinity and oxygen near 15°S in the west and 20°S in the east, suggesting the front is at the boundary between waters in the anticyclonic cell and the cyclonic cell south of it.

3. Tropical Circulation

First, the features of the AAIW in the subequatorial gyre suggested by the isopycnal maps in the previous section are further examined using the geostrophic flow and tracer fields along two meridional sections (Figure 6) as follows: 25°W south of 1°S from R/V *Melville* during April 1989 (Hydros 4) and along the Greenwich meridian from R/V *Knorr* during February–March 1988 (part of SAVE leg 3). Second, the flow of AAIW near the equator is discussed based on the tracer fields using these two meridional sections, crossing the equator near 25°W and 4°W, respectively, and four

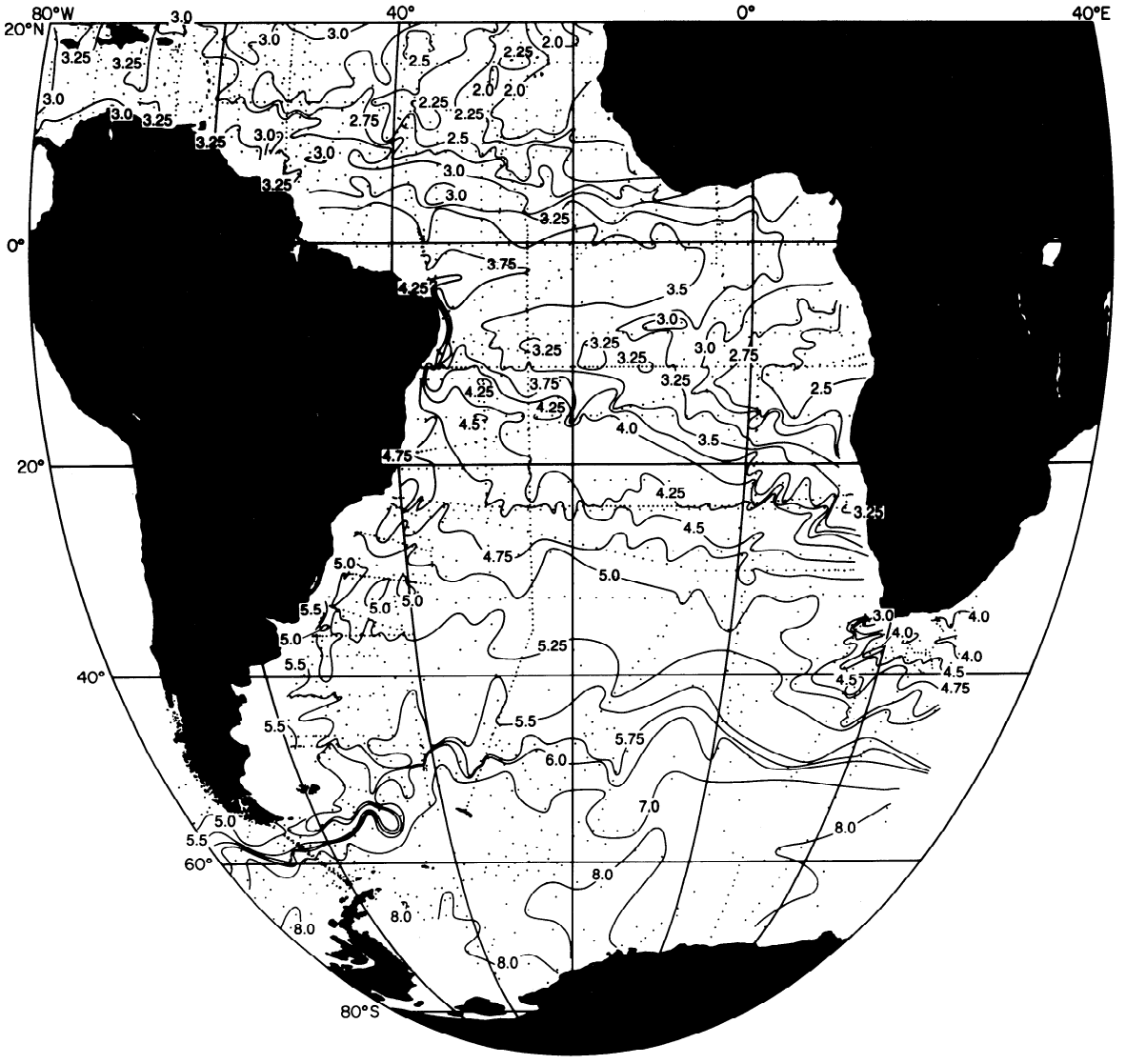

Figure 3. Oxygen (milliliters per liter) on the $27.3\sigma_\theta$ isopycnal.

others (Figure 6) as follows: crossing the equator near 35°W from R/V *Knorr* during August 1983, near 25°W from R/V *Oceanus* during August 1988 (part of OC202 [*Tsuchiya et al.*, 1992]), near 17.5°W from R/V *Knorr* during November–December 1987 (part of SAVE leg 1 or SAVE1), and near 0.5°W from R/V *Knorr* during December 1987 (part of SAVE leg 2 or SAVE2).

3.1. The Subequatorial Gyre

AAIW is recognized as a low-salinity tongue extending northward centered at 900 m near 30°S and at 700 m near the equator in meridional sections at 25°W and the Greenwich meridian (Figures 7b and 8b). The $27.3\sigma_\theta$ surface lies slightly below the core of the tongue south of about 20°S and just at the core north of it. A high-oxygen tongue of the AAIW (Figures 7c and 8c) also extends northward slightly above the low-salinity tongue but terminates near 20°S in both sections. In the description of the 25°W section of *Tsuchiya et al.* [1994] the northern termination of the AAIW oxygen maximum was shown to be related to the basin-scale circulation pattern of the AAIW. The isopleths of $27.3\sigma_\theta$ and denser (Figures 7a and 8a) generally deepen poleward, south of about 20°S, corresponding with a broad area of westward geostrophic flow relative to 3000 dbar in both sections (Figure 9): from the surface to 1500 dbar or deeper south of 21°S in the 25°W section and from the surface to 1000 dbar or deeper south of 22°S in the Greenwich meridian section. That is, the high-oxygen tongue is found in the area of the westward flow. This flow corresponds with the northern rim of the subtropical gyre and southern rim of the subequatorial gyre or the westward extension of the Benguela Current [*Stramma and Peterson*, 1989; *Peterson and Stramma*, 1991] as shown in the acceleration potential map (Figure 4).

Furthermore, the high-oxygen tongue of the AAIW has a meridional discontinuity in properties. At $27.3\sigma_\theta$ a front in salinity, oxygen, and nitrate occurs near 25°S in the 25°W section and near 28°S in the Greenwich meridian section (marked F1 in Figures 10–12). The front lies within the broad westward flow, although the local flow is slightly eastward at the center of the front in the Greenwich meridian section. As suggested by the isopycnal maps in section 2, this front is the boundary between the subtropical and subequatorial gyres

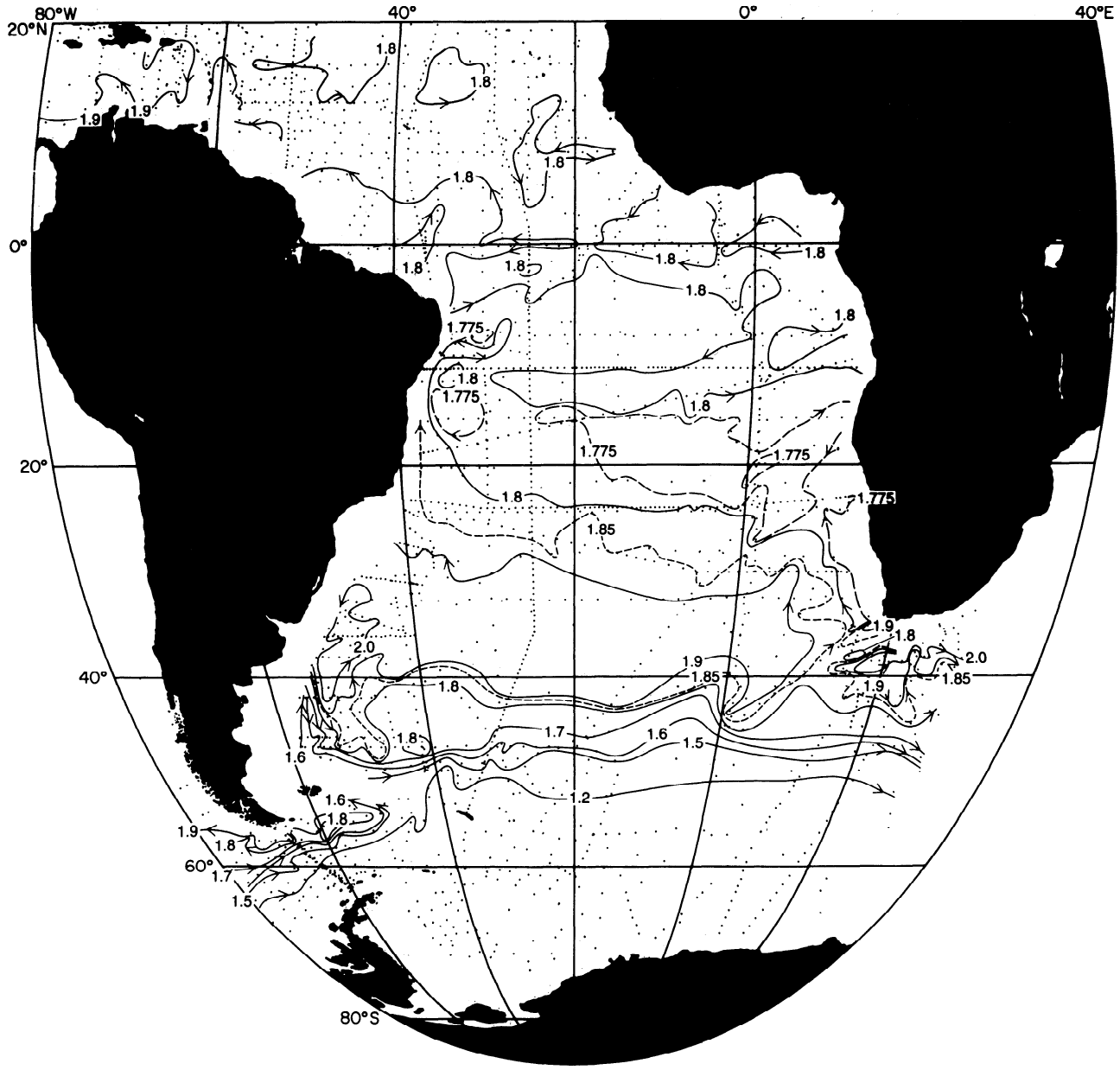

Figure 4. Acceleration potential (10 m^2 s^{-2}) on the 27.3σ_θ isopycnal relative to 3000 dbar.

and divides the AAIW in the high-oxygen tongue into two parts. The southern part is the newer AAIW circulating in the subtropical gyre, while the northern part is older and circulating in the subequatorial gyre.

A second front of salinity, oxygen, and nitrate appears at 27.3σ_θ within the subequatorial gyre, near 15°S in the 25°W section and near 21°S in the Greenwich meridian section (marked F2 in Figures 10–12); it is associated with the meridional maximum of the eastward geostrophic speeds. While this front is located within the large-scale cyclonic subequatorial gyre according to the previous studies, Figure 9 shows robust subsurface eastward speeds between 13°S and 16°S in the 25°W section and between 15°S and 22°S in the Greenwich meridian section. That is, the front is situated in the eastward flow and divides the AAIW into the following two parts: newer AAIW to the south and older AAIW to the north. These features of the second front in the synoptic sections agree well with the features in the isopycnal maps (Figures 2–4) discussed in section 2 and suggest that this front associated with the eastward flow lies at the boundary between an anticyclonic cell, carrying the older AAIW, and the cyclonic cell, carrying the newer AAIW, south of it.

The low-salinity tongue of the AAIW does not become more saline monotonically farther towards the north. There is a lateral maximum of salinity near 10°S in both sections (Figures 7b and 8b), which is also clearly demonstrated in the meridional plot of salinity at the vertical salinity minimum by *Tsuchiya et al.* [1994] for the 25°W section. Figure 10 shows that this meridional maximum appears also at 27.3σ_θ. There is a prominent oxygen minimum centered at about 400 m and at 15°S in the Greenwich meridian section (Figure 8c), which appears as a meridional oxygen minimum at 27.3σ_θ (Figure 11b). A less prominent and more patchy oxygen minimum occurs at about 400 m and around 7°S in

Figure 5. Potential vorticity (10^{-11} m^{-1} s^{-1}) on the 27.3σ_θ isopycnal.

the 25°W section (Figure 7c), which also appears as a meridional oxygen minimum at 27.3σ_θ (Figure 11a). A vertical maximum in nitrate also occurs at the corresponding latitudes but is deeper than the oxygen minimum in both sections (not shown here; see *Tsuchiya et al.* [1994] for the 25°W section). A meridional nitrate maximum is also found at 27.3σ_θ (Figure 12). As described in section 2, these lateral extrema of the AAIW properties result from consumption of oxygen and vertical mixing near the eastern boundary in the subequatorial gyre and the westward advection of the water affected by these processes. Moreover, rather patchy distribution of the property extrema, especially in the 25°W section, suggests the complexity of the zonal advection of AAIW in the tropics.

Geostrophic velocity sections relative to 3000 dbar (Figure 9) show alternating zonal flow with spatial scale of a couple of hundred kilometers, reaching 1500 dbar or deeper, north of 13°S in the 25°W section and north of 8°S in the Greenwich meridian section. The bands of westward flow have been considered as branches of the South Equatorial Current (SEC) and the bands of eastward flow as the South Equatorial Undercurrent (SEUC) near 5°S and the South Equatorial

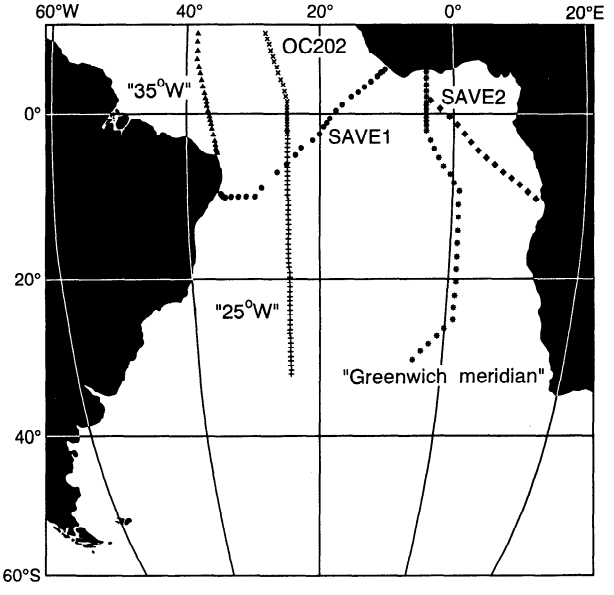

Figure 6. Locations of modern sections used.

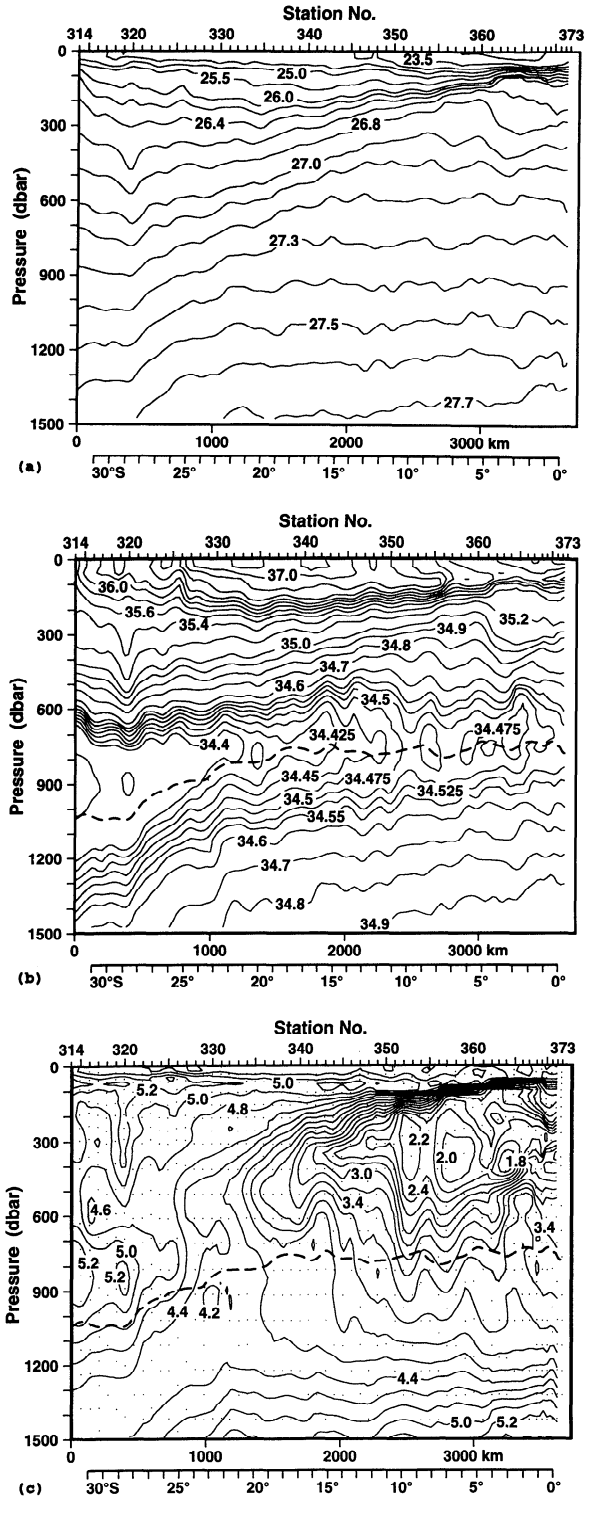

Figure 7. Vertical sections of (a) potential density σ_θ, (b) salinity (practical salinity units), and (c) oxygen (milliliters per liter) along 25°W. The potential density and salinity sections are based on conductivity-temperature-depth (CTD) data. The oxygen section is based on discrete bottle data indicated by dots. Dashed curves in the salinity and oxygen sections indicate the $27.3\sigma_\theta$ surface. The CTD stations were collected on the Hydros 4 expedition on R/V *Melville* in 1989 and were described by *Tsuchiya et al.* [1994].

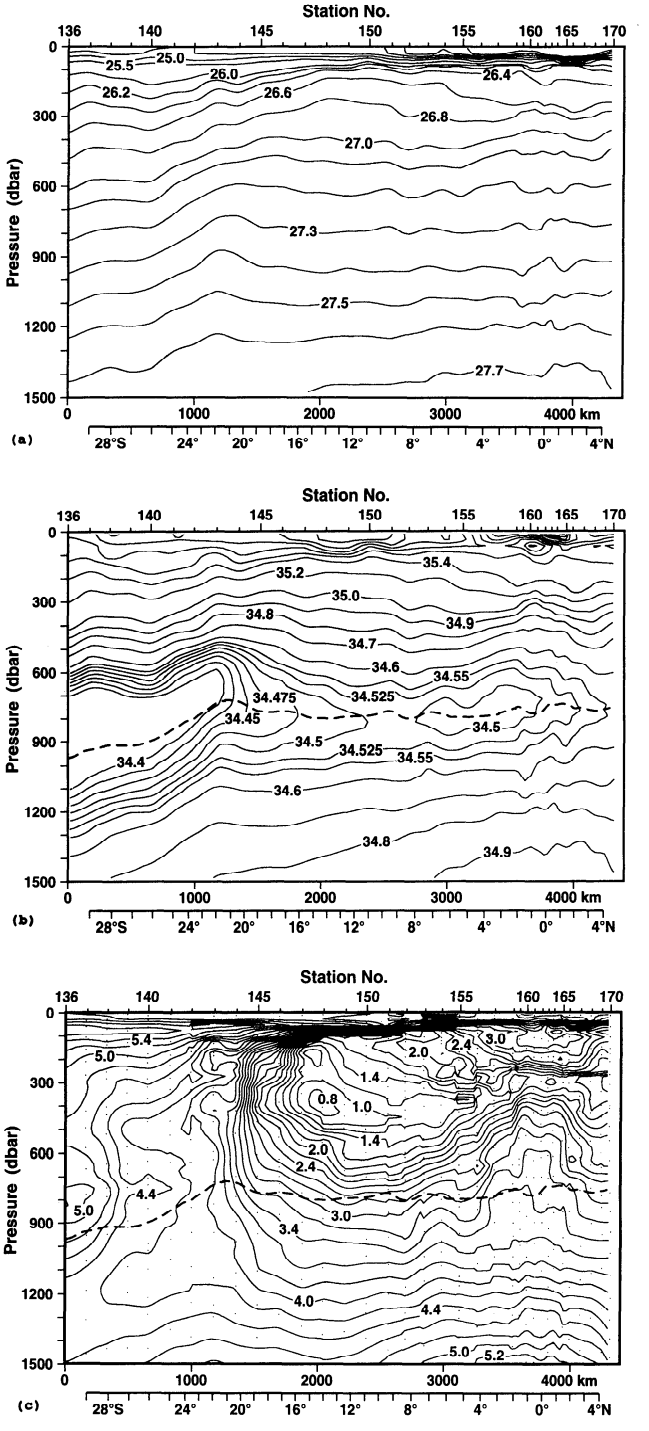

Figure 8. Same as Figure 7, but from the section near the Greenwich meridian. The CTD data were collected in 1988 as part of the South Atlantic Ventilation Experiment (SAVE) (leg 3 [*Scripps Institution of Oceanography*, 1992a]).

Countercurrent (SECC) near 8°S for the upper layer of the central Atlantic (see review by *Peterson and Stramma* [1991]). Figure 9 suggests that these currents also reach to intermediate depth and carry AAIW to the west and east.

As seen on the isopycnal maps (Figures 2–4), there appear lateral extrema of properties off Africa near 10°S. The Greenwich meridian section runs near the extremes. Most of the zonal speed maxima correspond with meridional extrema

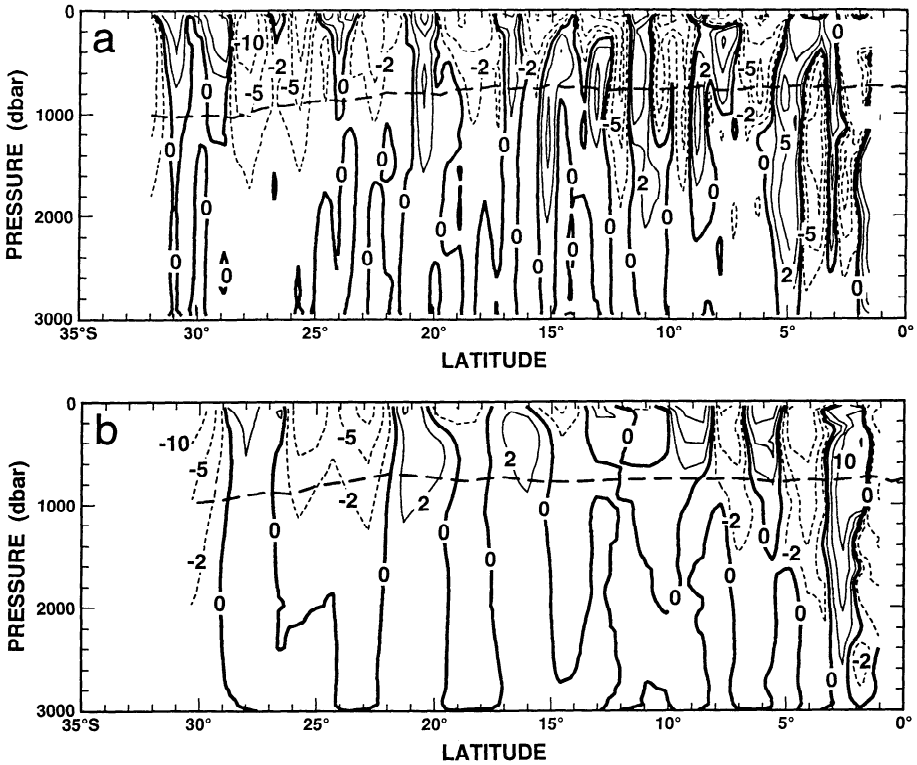

Figure 9. Vertical sections of geostrophic velocity (centimeters per second) relative to 3000 dbar at (a) 25°W and (b) the Greenwich meridian. Dashed contours indicate westward speeds. Thick dashed curves indicate $27.3\sigma_\theta$ surface. Average station spacing for 25°W was 65 km; for the Greenwich meridian it was 175 km, accounting for the difference in amount of lateral structure.

of isopycnal properties in the 25°W section. Maxima in salinity and nitrate and a minimum in oxygen are coincident near 10°S and 6–7°S, and are associated with meridional maxima of westward speeds (marked W in Figures 10–12). It is thus indicated that the westward flow carries the saline, oxygen-poor, and nitrate-rich AAIW from the east to the west. The westward flow is the northern part of the anticyclonic cell proposed in section 2. It is seen here that this cell includes at least two branches of westward flow. Coincident minima in salinity and nitrate and maxima in oxygen are found at 8–9°S and 5–6°S at $27.3\sigma_\theta$ in the 25°W section and are associated with meridional maxima of eastward speeds (marked E in Figures 10–12). Eastward advection of newer AAIW is thus suggested. The northern branch of the eastward flow may correspond with deep expression of the SEUC and the southern branch with SECC as reported by *Molinari* [1982] based on his meridional sections of geostrophic speed relative to 1000 dbar near 25°W. The present section shows the currents at the same latitude as his results and extending very deep.

The distributions of zonal speeds and properties are not as coincident farther east as at 25°W. The Greenwich meridian section runs near the core of saline, oxygen-poor, and nitrate-rich water off Africa, and its isopycnal properties instead show broad extrema between 5°S and 15°S. There is a sharp front in both oxygen and nitrate at 4°S (marked F3 in Figures 11 and 12) associated with westward flow on its south side. This feature most likely indicates the boundary between the anticyclonic cell and the cyclonic cell north of it. The two apparent branches of the eastward flow carrying the newer AAIW in the 25°W section, however, suggest that the northern cyclonic cell is more complicated than suggested by the isopycnal maps.

3.2. The Equatorial Circulation

A salinity front is found immediately south of the equator at 0–1°S along 35°W, at 2°S along 25°W and 17.5°W, and at 0–1°S along 4°W (Figure 13). At 4°W the front is considerably weaker. There is no apparent front south of the equator near the Greenwich meridian. Where there is a front, a meridional minimum of salinity occurs on its south side. A meridional maximum of oxygen occurs on the south side of the salinity front, with concentrations decreasing toward the east (Figure 14). The maximum at 4°W is much less obvious than those farther west. There is no clear maximum near 0.5°W. Meridional minima of nitrate coincide with the oxygen maxima at 35°W and 25°W, while no clear minimum appears farther east (not shown). These extrema south of the front demonstrate that the salinity front south of the equator is the northern boundary of an eastward flow, which carries newer AAIW from the western boundary at least as far east as 4°W.

Another salinity front is found immediately north of the equator at 1.5–2°N along 35°W, at 2–2.5°N along 25°W, at 1–2°N along 17.5°W, and at 2–3°N along 4°W. The front becomes less sharp toward the east. A meridional maximum of oxygen occurs on the south side of the salinity front at 35°W and 25°W, with concentrations decreasing toward the east. There is no clear maximum farther east. A meridional minimum of nitrate coincides with the oxygen maximum at 35°W and 25°W (not shown). These extrema indicate that the

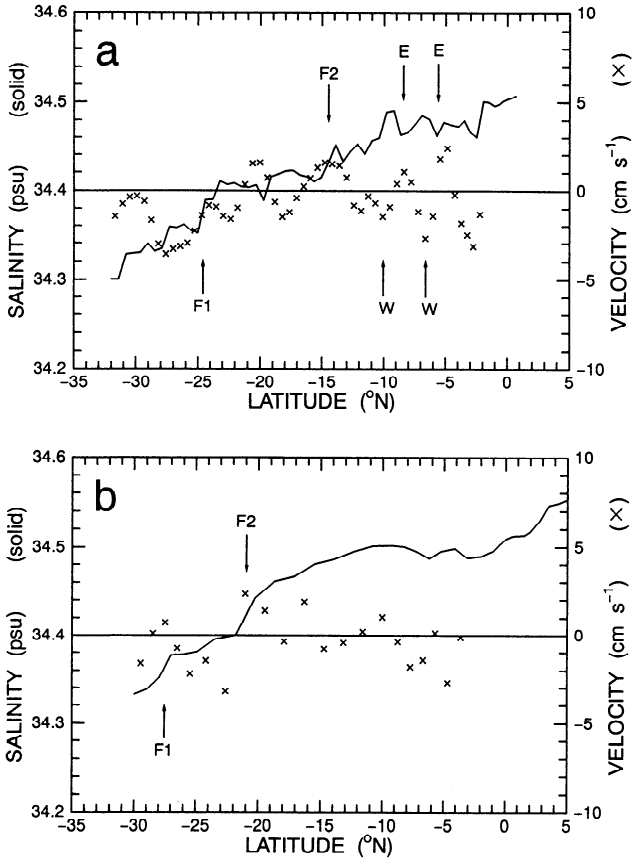

Figure 10. Salinity (solid curves) and geostrophic velocity (crosses) at $27.3\sigma_\theta$ along the (a) 25°W and (b) Greenwich meridian sections. Eastward velocity is positive. The geostrophic velocity was smoothed horizontally using a Gaussian filter with an e-folding scale of 100 km. F1 and F2 are the fronts referred to in the text. E and W indicate eastward and westward flows referred to in the text.

salinity front north of the equator is associated with another eastward flow on its south side, which extends at least as far east as 25°W and which carries newer AAIW from the western boundary.

Salinity is fairly homogeneous between the two fronts south and north of the equator, being more homogeneous along the western four sections than the eastern two. There are no significant and systematic zonal variations in salinity right on the equator. On the other hand, oxygen on the equator decreases to the east, while nitrate has no obvious zonal variation along the equator (not shown). The oxygen distribution along the equator suggests that the AAIW on the equator is newer in the west and becomes older to the east, while the other properties show no clear tendency.

Vertical profiles of salinity at the individual stations across the equator along the 25°W section are shown in Figure 15. Stations between 4°4′N and 2°42′N are north of the northern salinity front, and stations between 2°38′S and 3°2′S are south of the southern front. It is strikingly demonstrated that salinity between the two fronts, roughly between 2°S and 2°N and thus within the equatorial baroclinic deformation radius, is laterally homogeneous in the density range centered at $27.3\sigma_\theta$ (Figure 15a). This feature suggests that more lateral mixing occurs in this density range than at higher or lower density. It is also demonstrated that salinity is vertically homogeneous at 650–900 m depth between the two fronts, suggesting considerable vertical mixing (Figure 15b).

The features of the salinity, oxygen, and nitrate near the equator described above could be explained by the following three different types of flow on the equator at $27.3\sigma_\theta$: westward flow, eastward flow which is weaker than that to the north or south, or eastward flow with possibly large vertical mixing. *Richardson and Schmitz* [1993] showed a broad band, from 5°S to 6°N, of eastward flow at 800 m from the western boundary to at least 5°W using the SOFAR floats. The $27.3\sigma_\theta$ surface lies slightly above 800 m (Figures 1, 7, and 8). Their float trajectories also suggest possible divergence at the equator, which can be related to large vertical mixing. Thus their results support the suggestion of eastward flow with large vertical mixing on the equator. On the other hand, they presented a vertical profile of velocity at 30°W on the equator measured with a freely falling velocity profiler, showing alternating eastward and westward currents over the upper 2200 m. A prominent eastward current appears from 800 to 1400 m; a less prominent westward current occurs just above it, which possibly corresponds to the flow at $27.3\sigma_\theta$. Since Richardson and Schmitz estimated that all the floats probably sank about 100 m per year, their trajectories may have been influenced mainly by the east-

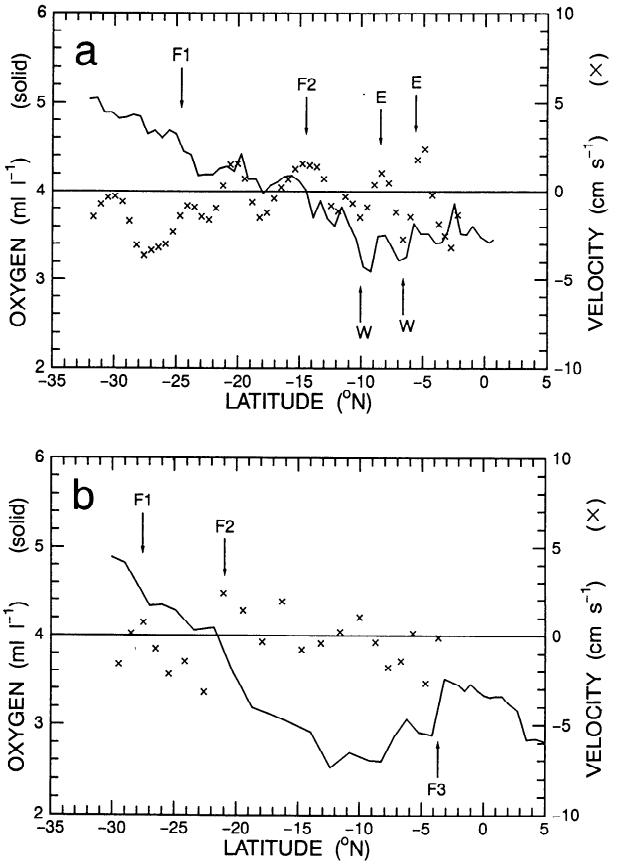

Figure 11. Oxygen (solid curves) and geostrophic velocity (crosses) at $27.3\sigma_\theta$ along the (a) 25°W and (b) Greenwich meridian sections. Eastward velocity is positive. The geostrophic velocity was smoothed as in Figure 10. F1, F2, and F3 are the fronts referred to in the text. E and W indicate eastward and westward flows referred to in the text.

ward flow below 800 m. Therefore westward flow on the equator cannot be ruled out by their results.

Böning and Schott [1993] discussed equatorial flow in a high-resolution, wind-driven, and thermohaline circulation model of the Atlantic Ocean. Although they concentrated on the deep layer, their meridional sections of velocity along 30°W show zonal currents of opposite directions above and below 700–900 m depth; they change direction seasonally. *Richardson and Schmitz* [1993] also suggested reversal of the direction of the equatorial flow at the end of the 21-month-long tracking period, although they show no seasonality. These temporal variations make it difficult to determine mean equatorial flow based on synoptic hydrography. The variations also may contribute to large lateral and vertical mixing along with possible divergence and large vertical and horizontal shears in the equatorial flow.

4. Conclusions and Remarks

Maps of the properties at $27.3\sigma_\theta$ corresponding to the AAIW salinity minimum north of 20°S were constructed using recent and historical data. Salinity and oxygen maps and acceleration potential support the view that a portion of the AAIW is advected northward all along the coast of Brazil as an intermediate western boundary flow [*Wüst*, 1935; *Zemba*, 1991] but that most of the AAIW which enters the tropics comes from the flow around the subtropical gyre [*Zemba*, 1991]. There appears a relatively high potential vorticity tongue extending northwestward along the northeastern rim of the subtropical gyre from the south of Africa, which supports influence from the Indian Ocean at the AAIW density as *Gordon et al.* [1992] argued. *Rintoul*'s [1991] inverse calculation showed no net transfer of AAIW from the Indian Ocean to the Atlantic Ocean. The two

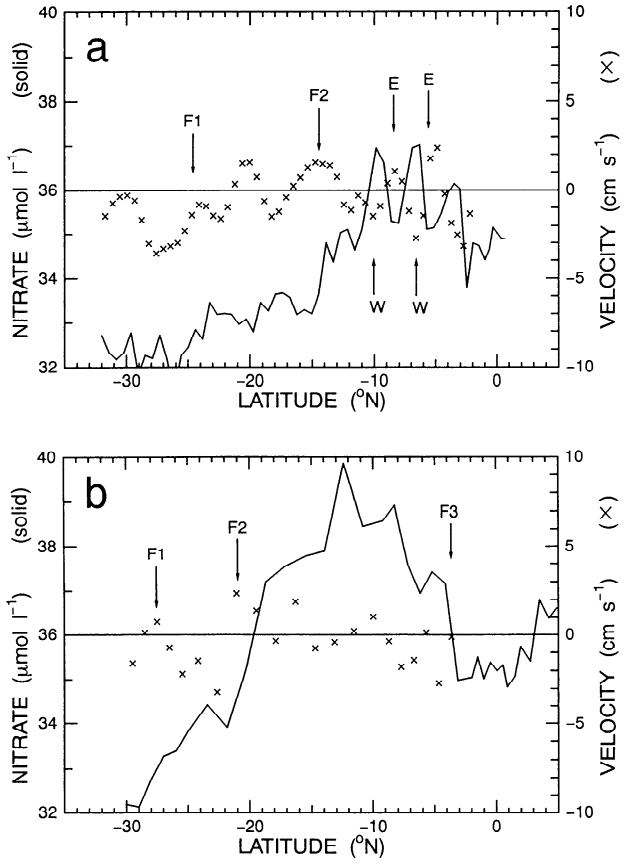

Figure 12. Nitrate (solid curves) and geostrophic velocity (crosses) at $27.3\sigma_\theta$ along the (a) 25°W and (b) Greenwich meridian sections. Eastward velocity is positive. The geostrophic velocity was smoothed as in Figure 10. F1, F2, and F3 are the fronts referred to in the text. E and W indicate eastward and westward flows referred to in the text.

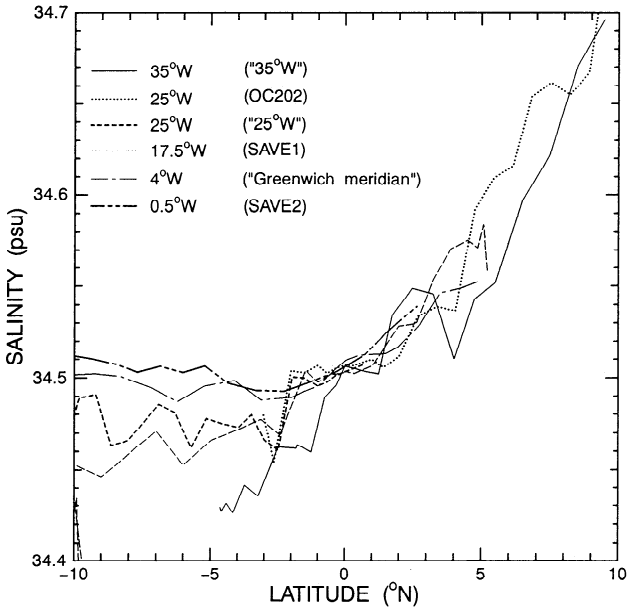

Figure 13. Salinity at $27.3\sigma_\theta$ across the equator along the sections at or near 35°W (R/V *Knorr* in 1983), 25°W (north of 3°S, R/V *Ocenus* OC202 in 1988; south of 1°S, R/V *Melville* Hydros 4 in 1989), 17.5°W (R/V *Knorr* SAVE leg 1 in 1987), 4°W (R/V *Knorr* SAVE leg 3 in 1988), and 0.5°W (R/V *Knorr* SAVE leg 2 in 1987).

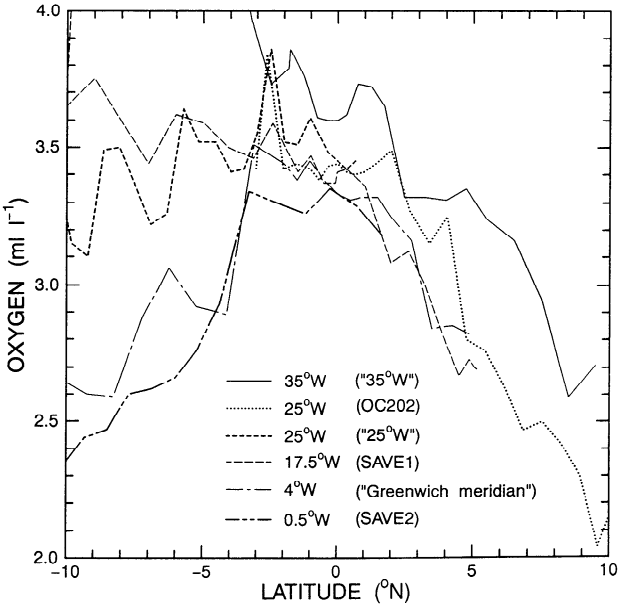

Figure 14. Same as Figure 13, but for oxygen.

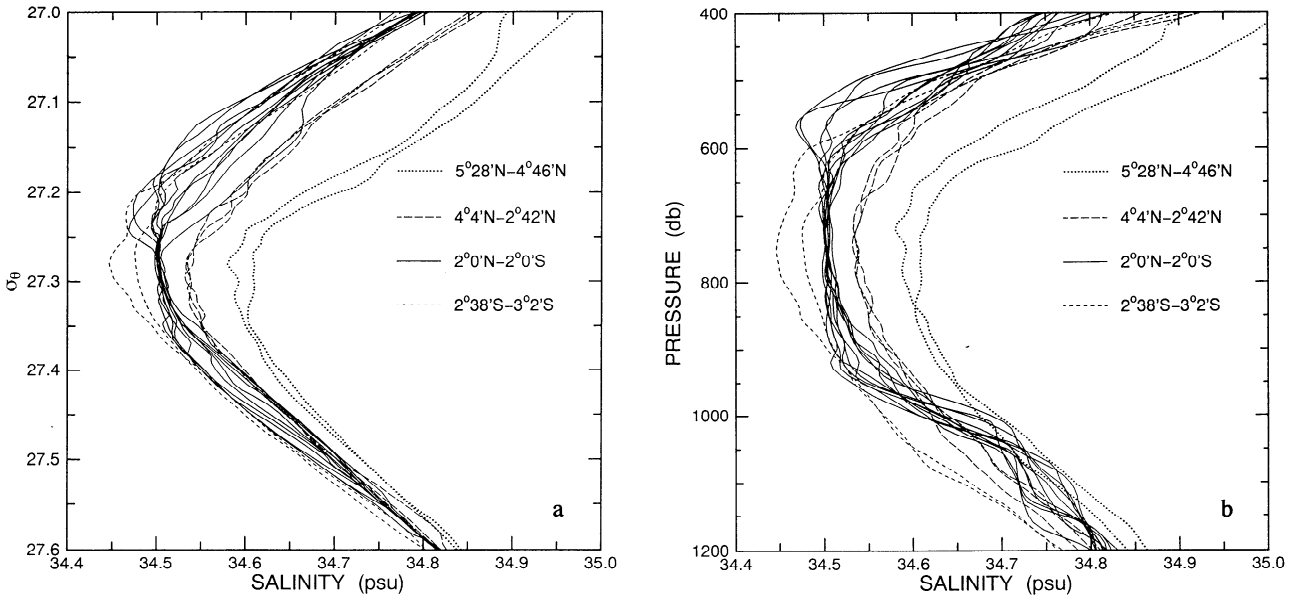

Figure 15. Vertical profiles of salinity using (a) σ_θ and (b) pressure as the vertical axis for each station near the equator from CTD stations at 25°W collected in 1988 on R/V *Oceanus* OC202 [*Tsuchiya et al.*, 1992] at 5°28′N–4°46′N (stations 107–108), at 4°4′N–2°42′N (stations 109–111), at 2°0′N–2°0′S (stations 112–122), and at 2°38′S–3°2′S (stations 123–124).

results do not conflict because the Indian AAIW can enter the Atlantic, affect the AAIW layer in the Atlantic through lateral and/or vertical mixing, and leave the Atlantic with no net AAIW transfer from the Indian Ocean to the Atlantic. The subequatorial gyre discussed in this paper could be a major site of such mixing.

In the cyclonic subequatorial gyre, high salinity is confirmed in the eastern tropical South Atlantic off Africa along with low oxygen and high nitrate, supporting that vertical mixing as well as biological processes alter the isopycnal properties. Acceleration potential at $27.3\sigma_\theta$ for the whole South Atlantic as well as geostrophic speeds and properties along 25°W and the Greenwich meridian indicate that the South Atlantic subequatorial gyre actually consists of the following three cells: the northern cyclonic cell centered at about 7°S, the southern cyclonic cell centered at about 19°S in the west and 23°S in the east, and the anticyclonic cell in between centered at about 13°S. Zonal flows associated with these cells account for the tongue and fronts in the AAIW properties. Coinciding fronts in salinity, oxygen, and nitrate at about 25°S in the west and near 30°S in the east are the boundary between the subtropical gyre and the subequatorial gyre (the southern cyclonic cell). Another front at about 15°S in the west and near 20°S in the east is the boundary between the southern cyclonic cell and the anticyclonic cell. It is noted that *Gordon and Bosley*'s [1991] map of dynamic topography at 500 dbar, shallower than the $27.3\sigma_\theta$ surface, relative to 1500 dbar also suggests two separate cyclonic cells in the eastern subequatorial South Atlantic, while the splitting of the cyclonic cell farther to the west cannot be evidenced owing to lack of data.

A low-salinity and high-oxygen tongue centered at 3–4°S extends eastward from the western boundary across the basin, indicating eastward advection of relatively new AAIW south of the equator. A weak tongue of low salinity is also found north of the equator centered at 1–2°N, also suggesting eastward flow carrying the AAIW immediately north of the equator. Robust eastward flow at the equator just below the $27.3\sigma_\theta$ surface is evident in the work of *Richardson and Schmitz* [1993]. On the basis of water properties, we conclude that the equatorial flow at $27.3\sigma_\theta$ is either eastward with large vertical mixing or westward.

Although the tracer fields indicate relatively new AAIW flowing eastward from the western boundary north of the equator, no clear signature of a cross-equatorial western boundary current is apparent in patterns of acceleration potential near the equator. The tracers also suggest that the AAIW north and south of the equator can affect each other through considerable lateral mixing. Slow leakage all along the equator might account for at least part of cross-equatorial transport of the AAIW. Further investigation of this and the above mentioned lateral and vertical mixing is required to construct a better picture of the AAIW circulation as a part of the meridional circulation cell.

Acknowledgments. This research was supported by grant OCE-9201315 from the National Science Foundation's Ocean Sciences Division to SIO. The SAVE and Hydros 4 data collection was also funded by NSF. T.S. was also financially supported by the Japanese Ministry of Education, Science, and Culture (Grant-in-Aid for Encouragement of Young Scientists, 06740365). We are grateful to Phil Richardson for making us aware of his float results and to M. Tsuchiya, J. Reid, and R. Peterson for stimulating discussions. We thank the Physical Oceanography Laboratory, Tohoku University, for allowing T.S. to visit SIO.

References

Böning, C. W., and F. A. Schott, Deep currents and eastward salinity tongue in the equatorial Atlantic: Results from an eddy-resolving, primitive equation model, *J. Geophys. Res.*, *98*, 6991–6999, 1993.

Broecker, W. S., and T. Takahashi, Hydrography of the central

Atlantic, IV, Intermediate waters of Antarctic origin, *Deep Sea Res., Part A, 28*, 177–193, 1981.

Buscaglia, J. L., On the circulation of the Intermediate Water in the southwestern Atlantic Ocean, *J. Mar. Res., 29*, 245–255, 1971.

Fine, R. A., Circulation of Antarctic Intermediate Water in the South Indian Ocean, *Deep Sea Res., Part I, 40*, 2021–2042, 1993.

Gordon, A. L., and K. T. Bosley, Cyclonic gyre in the tropical South Atlantic, *Deep Sea Res., Part A, 38*, suppl., 323–343, 1991.

Gordon, A. L., and A. R. Piola, Atlantic Ocean upper layer salinity budget, *J. Phys. Oceanogr., 13*, 1293–1300, 1983.

Gordon, A. L., R. F. Weiss, W. M. Smethie Jr., and M. J. Warner, Thermocline and Intermediate Water communication between the South Atlantic and Indian Oceans, *J. Geophys. Res., 97*, 7223–7240, 1992.

Keffer, T., The ventilation of the world's oceans: Maps of the potential vorticity fields, *J. Phys. Oceanogr., 15*, 509–523, 1985.

McCartney, M., Subantarctic mode water, in A Voyage of Discovery: George Deacon 70th Anniversary Volume, *Deep Sea Res.*, suppl., 103–119, 1977.

McCartney, M., The subtropical recirculation of mode waters, *J. Mar. Res., 40*, suppl., 427–464, 1982.

Molinari, R. L., Observations of eastward currents in the tropical South Atlantic Ocean: 1978–1980, *J. Geophys. Res., 87*, 9707–9714, 1982.

Molinelli, E. J., The antarctic influence on Antarctic Intermediate Water, *J. Mar. Res., 39*, 267–293, 1981.

Peterson, R. G., and L. Stramma, Upper-level circulation in the South Atlantic Ocean, *Prog. Oceanogr., 26*, 1–73, 1991.

Piola, A. R., and D. T. Georgi, Circumpolar properties of antarctic intermediate and subantarctic mode water, *Deep Sea Res., Part A, 29*, 687–711, 1982.

Reid, J. L., Intermediate waters of the Pacific Ocean, *John Hopkins Oceanogr. Stud., 2*, 85 pp., 1965.

Reid, J. L., On the middepth circulation and salinity field in the North Atlantic Ocean, *J. Geophys. Res., 83*, 5063–5067, 1978.

Reid, J. L., On the total geostrophic circulation of the South Atlantic Ocean: Flow patterns, tracers, and transports, *Prog. Oceanogr., 23*, 149–244, 1989.

Reid, J. L., On the total geostrophic circulation of the North Atlantic Ocean: Flow patterns, tracers, and transport, *Prog. Oceanogr., 33*, 1–92, 1994.

Richardson, P. L., and W. J. Schmitz Jr., Deep cross-equatorial flow in the Atlantic measured with SOFAR floats, *J. Geophys. Res., 98*, 8371–8388, 1993.

Rintoul, S. R., South Atlantic interbasin exchange, *J. Geophys. Res., 96*, 2675–2692, 1991.

Scripps Institution of Oceanography, South Atlantic Ventilation Experiment: Chemical, physical and CTD data report, Leg 1, Leg 2, Leg 3, *SIO Ref. 92-9*, 729 pp., Univ. of Calif., San Diego, 1992a.

Scripps Institution of Oceanography, South Atlantic Ventilation Experiment: Chemical, physical and CTD data report, Leg 4, 7 December 1988–15 January 1989, Leg 5, 23 January–8 March 1989, R/V *Melville*, *SIO Ref. 92-10*, 625 pp., Univ. of Calif., San Diego, 1992b.

Scripps Institution of Oceanography, Hydros Leg 4: Physical, chemical, and CTD data, 13 March–19 April 1989, R/V *Melville*, *SIO Ref. 92-12*, 190 pp., Univ. of Calif., San Diego, 1992c.

Stramma, L., and R. G. Peterson, Geostrophic transport in the Benguela Current region, *J. Phys. Oceanogr., 19*, 1440–1448, 1989.

Taft, B. A., Distribution of salinity and dissolved oxygen on surfaces of uniform potential specific volume in the South Atlantic, South Pacific and Indian Oceans, *J. Mar. Res., 21*, 129–146, 1963.

Tsuchiya, M., Circulation of the Antarctic Intermediate Water in the North Atlantic Ocean, *J. Mar. Res., 47*, 747–755, 1989.

Tsuchiya, M., Flow path of the Antarctic Intermediate Water in the western equatorial South Pacific Ocean, *Deep Sea Res., Part A, 38*, suppl., S273–S279, 1991.

Tsuchiya, M., L. D. Talley, and M. S. McCartney, An eastern Atlantic section from Iceland southward across the equator, *Deep Sea Res., Part A, 39*, 1885–1917, 1992.

Tsuchiya, M., L. D. Talley, and M. S. McCartney, Water-mass distributions in the western South Atlantic; A section from South Georgia Island (54°S) northward across the equator, *J. Mar. Res., 52*, 55–81, 1994.

Warner, M. J., and R. F. Weiss, Chlorofluoromethanes in South Atlantic Antarctic Intermediate Water, *Deep Sea Res., Part A, 39*, 2053–2075, 1992.

Wüst, G., Die Stratosphäre, *Wiss. Ergeb. Dtsch. Atl. Exped., 6*(1/2), 109–288, 1935.

Zemba, J. C., The structure and transport of the Brazil Current between 27° and 36° south, Ph.D. thesis, *WHOI-91-37*, 160 pp., Woods Hole Oceanogr. Inst./Mass. Inst. of Technol., Woods Hole, Mass., 1991.

T. Suga, Department of Geophysics, Graduate School of Science, Tohoku University, Aoba ku, Sendai 980-77, Japan (e-mail: suga@pol.geophys.tohoku.ac.jp).

L. D. Talley, Scripps Institution of Oceanography, University of California, San Diego, La Jolla, CA 92093-0230. (e-mail: ltalley@ucsd.edu)

(Received December 13, 1993; revised February 1, 1995; accepted February 23, 1995.)